MADRID
inter.noise 2019
June 16 - 19
NOISE CONTROL FOR A BETTER ENVIRONMENT

Localization of Noise Sources in an Outdoor HVAC Unit by using the Arbitrary Source Location Method in Combination with Wideband Acoustical Holography

Lepak, WeSaam[1]
Sung, Weonchan[2]
Shi, Tongyang[3]
Liu, Yangfan[4]
Thor, Weimin[5]
Davies, Patricia[6]
Bolton, J. Stuart[7]

Ray W. Herrick Laboratories
Purdue University
177 S Russell St.
West Lafayette, IN 47907-2099

ABSTRACT

An outdoor heating, ventilating, and air conditioning (HVAC) unit has multiple noise sources which contribute to its overall acoustical signature, such as fan blade passage noise, compressor noise, aeroacoustic noise from vortex shedding off the grille, and structure-borne radiated noise. The identification of each noise source's strength and frequency content is key to giving the designer the ability to shape the HVAC unit's sound quality. In the present work, a two-dimensional microphone array was used to localize noise sources by using one of the commonly available acoustical holography methods, Wideband Acoustical Holography (WBH). It has previously been found that WBH holography results are very sensitive to the initial estimate of the equivalent source strengths, particularly at low frequencies. Here, a procedure referred to as the Arbitrary Source Location (ASL) model is introduced to provide the initial estimate of the principal source locations. It will be shown that when the latter procedure is combined with WBH, good sound field reconstructions and source visualizations may be achieved at relatively low frequencies, and that closely-spaced sources may be distinguished. The combined procedures will be illustrated through an application to noise source identification in an outdoor HVAC unit.

Keywords: Acoustic, Holography, HVAC
I-INCE Classification of Subject Number: 76

[1] wlepak@purdue.edu
[2] sung26@purdue.edu
[3] shi247@purdue.edu
[4] liu278@purdue.edu
[5] wthor@purdue.edu
[6] daviesp@purdue.edu
[7] bolton@purdue.edu

1. BACKGROUND

Noise from outdoor heating, ventilating, and air conditioning (HVAC) units is one of the major contributors to a building's interior and exterior background noise level. HVAC unit noise may lead to annoyance, irritation, and low speech intelligibility, which is particularly detrimental to conference room and classroom acoustic performance. At night, high HVAC unit noise can cause sleep disturbance, leading to an elevated risk of impaired cardiovascular health. The World Health Organization identifies sleep disturbance and annoyance as adverse health effects. Quiet HVAC units are also desired by consumers due to their perceived sense of being of a higher quality. Due to the importance of decreasing annoyance and increasing product quality, there is an engineering demand for sound optimization.

The acoustical signature of a product can be optimized by using an experiment-based, source-path model approach, consisting of a knowledge of source locations, source strengths, spectral content, and transfer paths. This type of model should have the capability to predict the sound level and spectral content at any receiver location in space, in any reverberant environment, at different HVAC operating conditions.

An HVAC unit has multiple noise sources which contribute to its overall acoustical signature, such as fan blade passage noise, compressor noise, aeroacoustic noise from vortex shedding off the grille, and structure-borne radiated noise. Once the fundamental physics of a specific HVAC unit has been investigated, the unit's individual machinery and mechanical processes can be connected to sound level, spectral characteristics, and acoustic directionality. To predict sound quality, the predicted sound from the source-path model can be passed through a sound quality model, that comprises multiple sound quality metrics, such as loudness, fluctuation, tonality, and impulsiveness, that together determines a final annoyance or product rating as perceived by a listener. The simultaneous use of a source-path model and a sound quality model enables the engineer to design an HVAC unit virtually to achieve high sound quality without the need of extensive prototyping.

The first step in this process is the ability to visualize the relevant sound sources so that they can then be modeled effectively. The focus of the present work was to develop those visualization procedures as described in the following sections.

2. SOUND VISUALIZATION METHODS

A two-dimensional microphone array can be used to localize noise sources by using one of the commonly available acoustical holography methods: e.g., Wideband Acoustical Holography (WBH) [1]. It has been shown that WBH results are very sensitive to the initial estimate of the source strengths, particularly at low frequencies [2,3]. A procedure referred to as the Arbitrary Source Location (ASL) model is introduced here to provide the initial estimate of the principal source locations and equivalent source strengths. It will be shown that when the latter procedure is combined with WBH, good sound field reconstructions and source visualizations may be achieved at relatively low frequencies, and that closely-spaced sources may be distinguished.

2.1 WIDEBAND ACOUSTICAL HOLOGRAPHY (WBH)

Wideband Acoustical Holography (WBH) is a parametric holography procedure which uses microphone signals measured on one surface to predict the sound pressure at any other location.

WBH's algorithm is based on reconstructing the sound pressure at the measurement location by using already known source locations and source strengths which are positioned on an equivalent source plane. The predicted sound pressure is then compared to the measured sound pressure. If the error is more than a preset threshold, then the algorithm updates the source strengths and iterates until the error is small. Once the error is small, the identified equivalent source distributions can be used to reconstruct the sound field at any other location, which will generate approximately the same sound field as the actual physical source, and hence allows the sound field to be back-projected to visualize the source distribution. This process is summarized in the flow chart in Fig. 1.

The accuracy of the required initial input to WBH, which is a collection of source locations and source strengths on an equivalent source plane, is critical to achieving accurate sound field reconstructions, as spatially depicted in Fig. 2. The Arbitrary Source Location (ASL) model described next, is used to obtain good initial inputs to the WBH procedure. The initial value of the monopole strengths on the equivalent source plane for WBH can be obtained by calculating the normal particle velocity of the sound field at those locations by using the output of the ASL model.

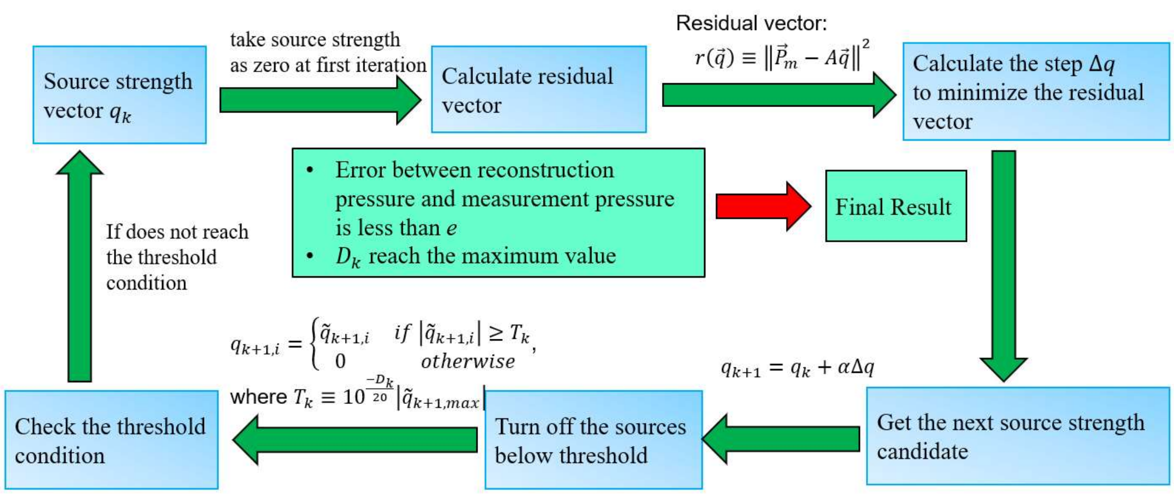

Figure 1: Flow chart of the Wibeband Acoustic Holography (WBH) Algorithm [3].

2.2 ARBITRARY SOURCE LOCATION (ASL) MODEL

The Arbitrary Source Location (ASL) model is a type of parametric, equivalent source model where the physically complex noise sources are represented by a small number of equivalent sources with undetermined source strengths and source locations in 3D space. This type of approach was recently developed by Liu and Bolton [4,5] and was applied in acoustical holography simulations by using higher order sources (multipoles) as the equivalent sources [6]. However, in general, the choice of equivalent sources can be monopoles, dipoles, quadrupoles, multipoles, or any combination of source types. In the current work, a distribution of monopoles were used to represent the actual sources in the ASL model, which were then used to generate an initial guess for WBH.

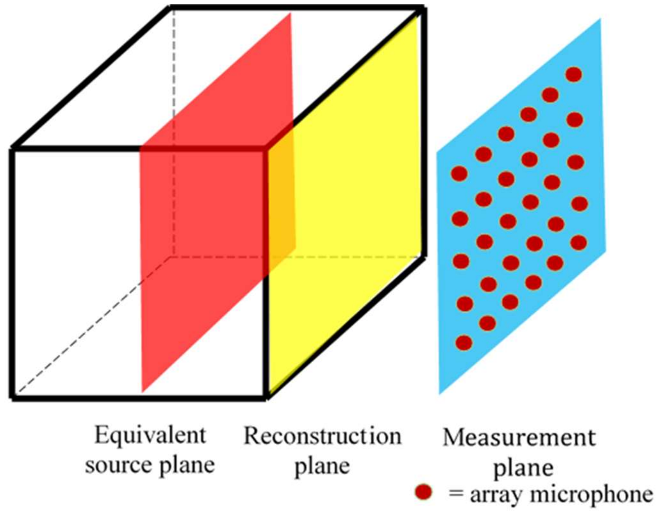

Figure 2: Spatial relation of measurement plane, reconstruction plane, and equivalent source plane as used in WBH measurements.

In the context of the ASL model, Fig. 3 shows how the physical sources can be represented by a relatively small number of equivalent monopoles (seven in Fig. 3), where $\vec{s_i} = \left(s_i^x, s_i^y, s_i^z\right)$ denotes the x, y, z coordinates of the i^{th} monopole. The locations and strengths of these equivalent sources were then calculated by using data measured from an array of microphones. The coordinates of the n^{th} microphone is denoted as $\overrightarrow{m_n} = (m_n^x,\ m_n^y, m_n^z)$.

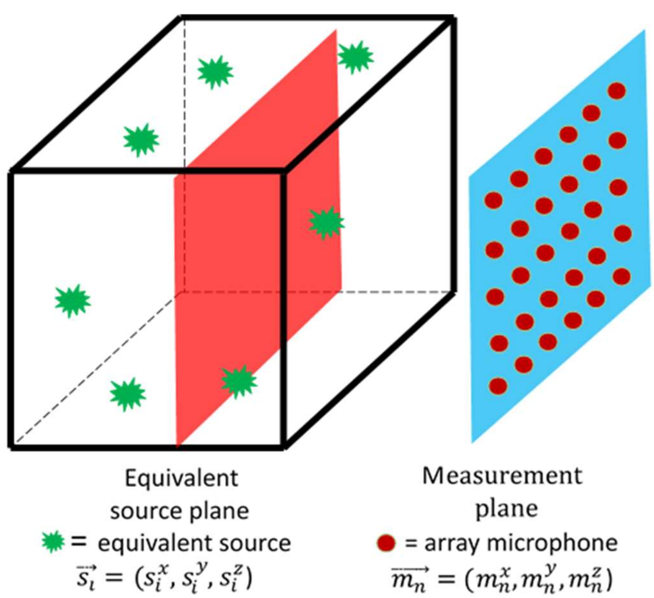

Figure 3: Spatial relation of the equivalent source plane, measurement plane, and the ASL model equivalent sources.

These individual equivalent sources are related to the total sound pressure at the measurement locations by:

$$p(\overrightarrow{m_n}) = \sum_i Q_i A_{in} \tag{1}$$

where $p(\overrightarrow{m_n})$ denotes the sound pressure at the n^{th} measurement location; Q_i denotes the strength of the i^{th} equivalent source; and A_{in} denotes the sound pressure expression of the i^{th} source at the n^{th} measurement location.

Since monopoles were chosen as the equivalent sources in the current work, A_{in} is only a function of the distance between the source and the measurement locations (denoted as r_{in} here) and can be expressed as:

$$A_{in} = \frac{e^{-jkr_{in}}}{4\pi r_{in}} \tag{2}$$

where

$$r_{in} = \sqrt{(s_i^x - m_n^x)^2 + \left(s_i^y - m_n^y\right)^2 + (s_i^z - m_n^z)^2} \tag{3}$$

and where k represents the wavenumber and $j = \sqrt{-1}$.

In the ASL model, the source locations are calculated by a non-linear optimization procedure and the source strengths are calculated via linear optimization [5]. Thus, the procedure requires an initial input of the number of equivalent sources included in the model, as well as the initial guess of their respective source locations. In the current work, the ASL algorithm was used to calculate the equivalent monopole strengths $Q_i{}'s$ and their locations $\vec{s_i}{}'s$ by minimizing the squared value of the error between the predicted and the measured sound pressure at the measurement locations $\overrightarrow{m_n}{}'s$: i.e., it is desired to minimize the value of:

$$\sum_n \left[p(m_n) - \sum_i Q_i A_{in}\right]^2 \tag{4}$$

where $p(m_n)$ is the measured sound pressure and $\sum_i Q_i A_{in}$ is the predicted sound pressure at the n^{th} measurement location. The algorithm used to solve the above non-linear least-square problem is the same as that implemented in ref. [5].

Once the source locations and strengths have been calculated, the sound pressure can be predicted at any position in space by using Eq. 1, with $\overrightarrow{m_n}$ replaced by the coordinates of the prediction location. The particle velocity in the *x*, *y*, and *z* directions are then expressed as:

$$v_x = -\frac{1}{j\omega\rho_o}\frac{\partial}{\partial r_{in}} p(\overrightarrow{m_n}) \frac{\partial r_{in}}{\partial m_n^x} \tag{5}$$

$$v_y = -\frac{1}{j\omega\rho_o}\frac{\partial}{\partial r_{in}} p(\overrightarrow{m_n}) \frac{\partial r_{in}}{\partial m_n^y} \tag{6}$$

$$v_z = -\frac{1}{j\omega\rho_o}\frac{\partial}{\partial r_{in}} p(\overrightarrow{m_n}) \frac{\partial r_{in}}{\partial m_n^z} \tag{7}$$

where ρ_o is the density of air. The reconstructed acoustic intensity, W/m^2, can then be calculated as:

$$I = \frac{1}{2}\mathrm{Re}\{PV^*\} \tag{8}$$

where $\mathrm{Re}\{\}$ denotes the real part of a complex quantity, and V^* is the complex conjugate of the particle velocity normal to the plane of interest.

The output of the ASL model is used to calculate the initial values of the monopoles distributed on the equivalent source plane shown in red in Figs. 2 and 3. The latter are then used as the starting point for the WBH procedure.

2.3 ACOUSTIC INTENSITY MEASUREMENT

Acoustic intensity measurements were used to verify and validate the results obtained through the above acoustical holography procedures. This was done via the use of a sound intensity probe kit (Type 2683 Dual Pre-amplifier and a pair of Type 4197 Microphones) supplied by Brüel and Kjær. The probe was mounted onto a mechatronic device which scanned across the side of the HVAC unit. The spatial resolution of the measurement grid was chosen to be smaller than half the wavelength corresponding to the maximum frequency of interest.

Acoustic intensity measurements identify the intensity hotspots on the unit to visualize source strengths and source locations. However, this method has the drawback that it can take many hours to perform a high-resolution scan across the unit. Acoustical holography methods were developed to reconstruct the sound field by using microphone array measurements, which can be completed in seconds or minutes, and thus offer a much faster approach to noise source identification.

3. EXPERIMENTAL RESULTS

As shown in Fig. 4, an 8 x 7 microphone array (56 microphones) was constructed to record the sound pressure on the measurement plane, 10 cm away from the side of the HVAC unit. The distance between each row was 6.5 cm while the distance between each column was 4 cm. The HVAC unit of interest was an outdoor variable speed residential unit which can be run with its fan only or run with both its fan and compressor operating.

The ASL algorithm was used to create 3025 monopole equivalent sources (2 cm between each monopole) on the equivalent source plane (red plane in Fig. 4) placed 2 cm behind the surface of the unit. That monopole array acted as the input to the WBH algorithm, which then reconstructed the sound field on the unit's surface by predicting the sound pressure, particle velocity, or acoustic intensity at 3025 points (2 cm between each point) on the reconstruction plane (yellow plane in Fig. 4).

A partial field decomposition (PFD) was first performed to separate the uncorrelated sound sources by singular value decomposition (SVD) [7]. In Figs. 5 and 6, the red line is the power spectral density (PSD) of the total sound field while the other 56 lines are the power spectral densities of each decomposed partial field. In Fig. 5, the data is for the case when the fan was run at 900 rpm while the compressor was run at 4250 rpm. In the case shown in Fig. 6, only the fan was running at 900 rpm, corresponding to a blade passage frequency of 45 Hz.

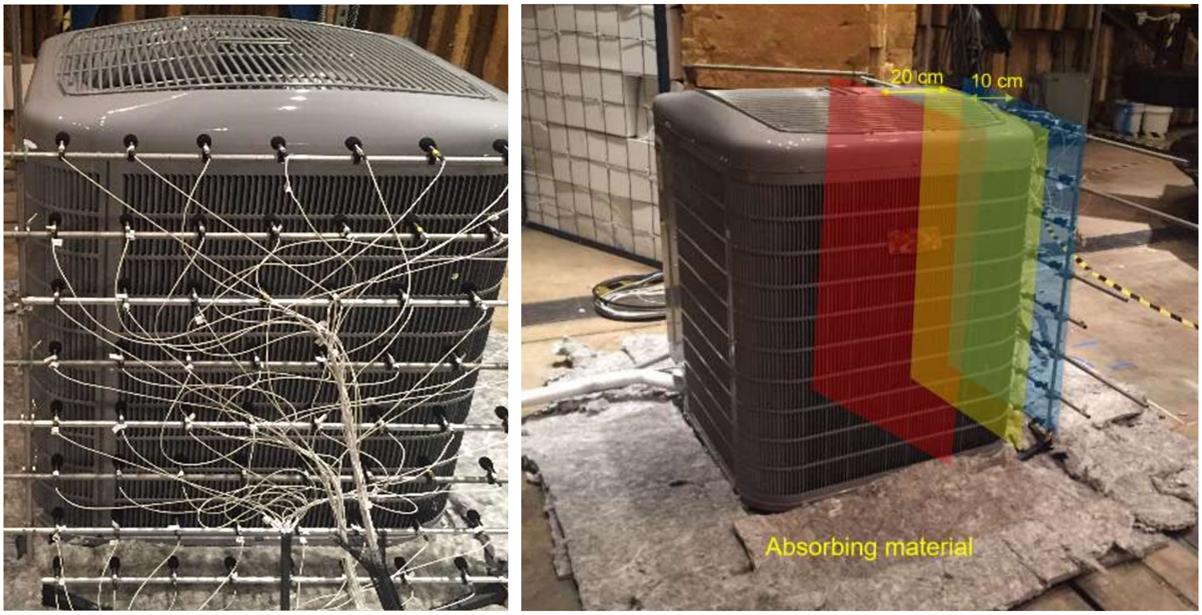

Figure 4: 8 x 7 microphone array (56 microphones) measuring an HVAC unit's sound pressure on the measurement plane (blue plane).

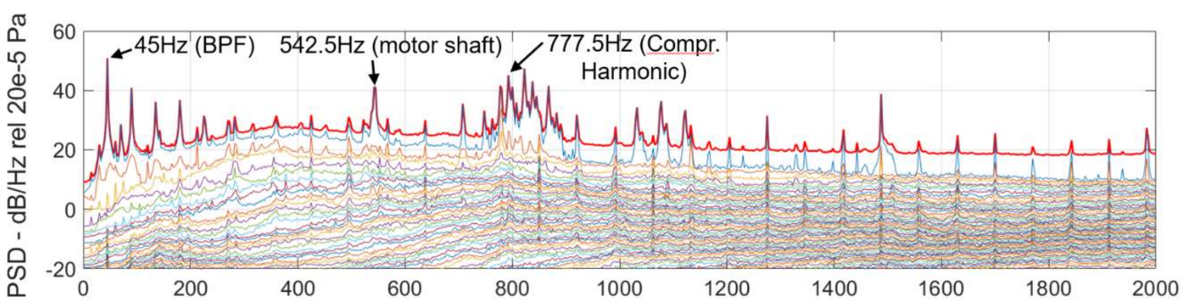

Figure 5: Fan and compressor running: power spectral density partial field decomposition when both the fan and compressor are running, A-weighted.

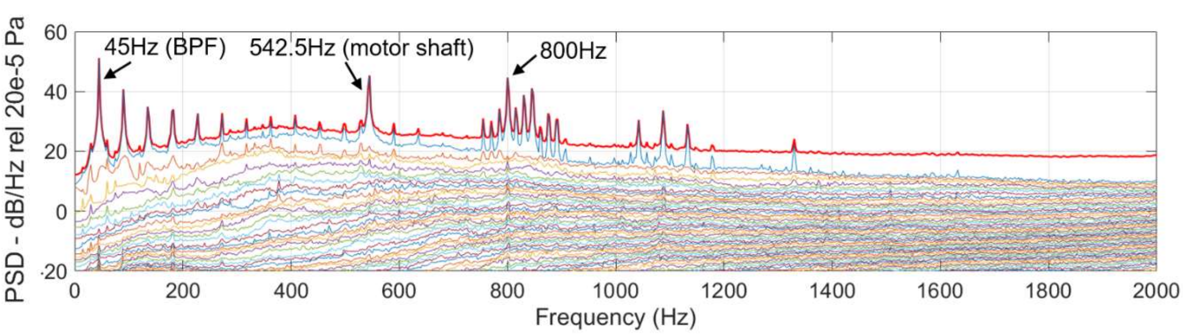

Figure 6: Only fan running: power spectral density partial field decomposition when only the fan is running, A-weighted.

When both the fan and compressor were running, fan harmonics and compressor harmonics can be seen at integer multiples of their fundamental frequency. In Fig. 6, of course, the compressor harmonics are absent in the case when only the fan was running. At all of these harmonics, the 1st partial field (blue line) is close to the total sound field (red line). This indicates that the sound pressure is dominated by one uncorrelated sound source. In the broad regions between the harmonics, the distance between the total sound field and the 1st partial field is large, indicating that the total sound field is the result of multiple contributing, uncorrelated noise sources.

The sound field was reconstructed at selected frequencies of interest, including the fan blade passage frequency (45 Hz), the 36th harmonic of the motor (542.5 Hz), the 11th harmonic of the compressor (777.5 Hz), and another, higher frequency noise source (800 Hz). The fan is at the top of the unit, the motor is centrally located above the fan, and the compressor is positioned at the bottom of the unit.

In Fig. 7, it can be seen that the fan is successfully localized at the top of the unit at its blade passage frequency (45 Hz). The motor's 1st partial field (542.5 Hz) is interestingly localized near the bottom of the unit. This suggests that the motor at the top of the unit is causing structural vibration throughout the unit, which then radiates as sound from the bottom of the unit. The motor's 2nd partial field is localized near the motor at the top of the unit.

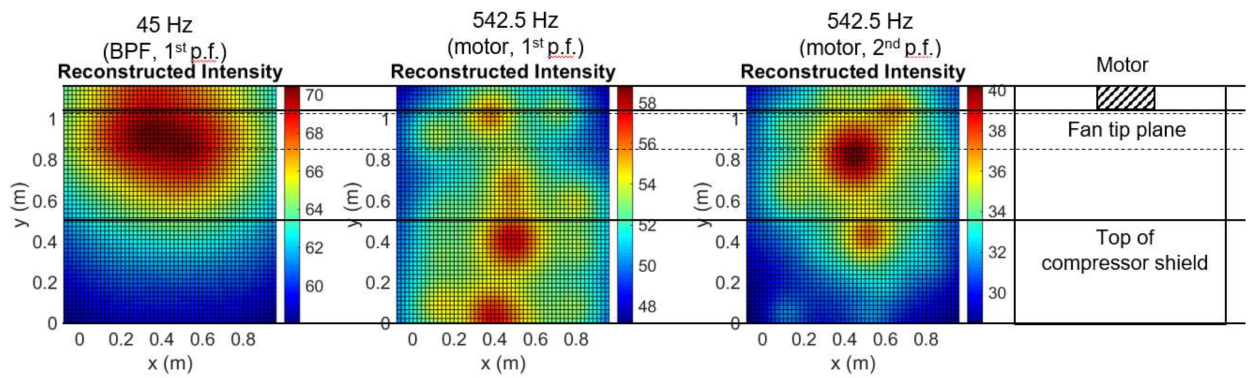

Figure 7: Fan and compressor running: reconstructed sound field of the 1st partial field at the blade passage frequency (45 Hz) and of the 1st and 2nd partial field at a motor harmonic frequency (542.5 Hz).

In Fig. 8, the sound field at these same frequencies were reconstructed for the case when only the fan was running. The results were very similar to those in Fig. 7, though the reconstruction of the 2nd partial field at 542.5 Hz was slightly better defined. Thus, it can be concluded that the majority of the noise visible in the Fig. 7 results is due to the operation of the motor and the fan.

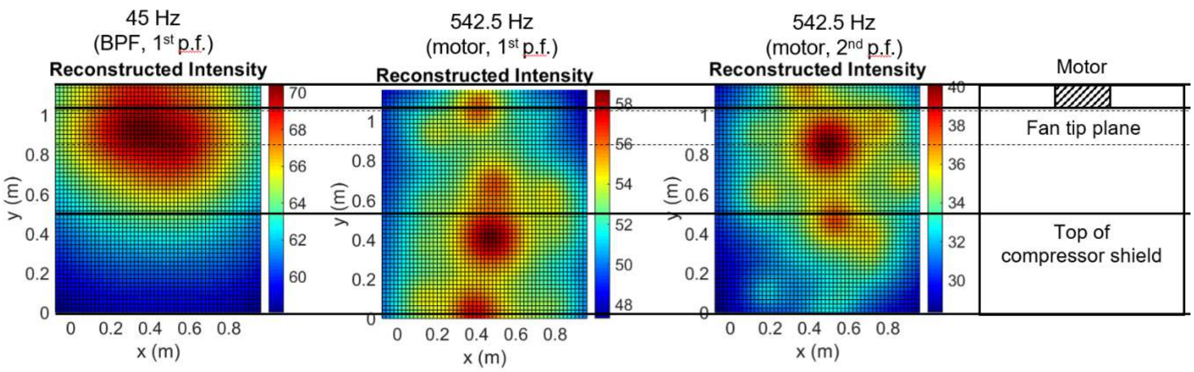

Figure 8: Only fan running: reconstructed sound field of the 1st partial field at the blade passage frequency (45 Hz) and of the 1st and 2nd partial field at a motor harmonic frequency (542.5 Hz).

Fig. 9 depicts the sound field reconstruction of the first three partial fields at the 11th harmonic of the compressor (777.5 Hz). The compressor is spatially located at the bottom of the unit, which was localized by the 2nd partial field. The 1st and 3rd partial fields localized the sound source at the top of the unit, possibly due to a structure-borne radiating source.

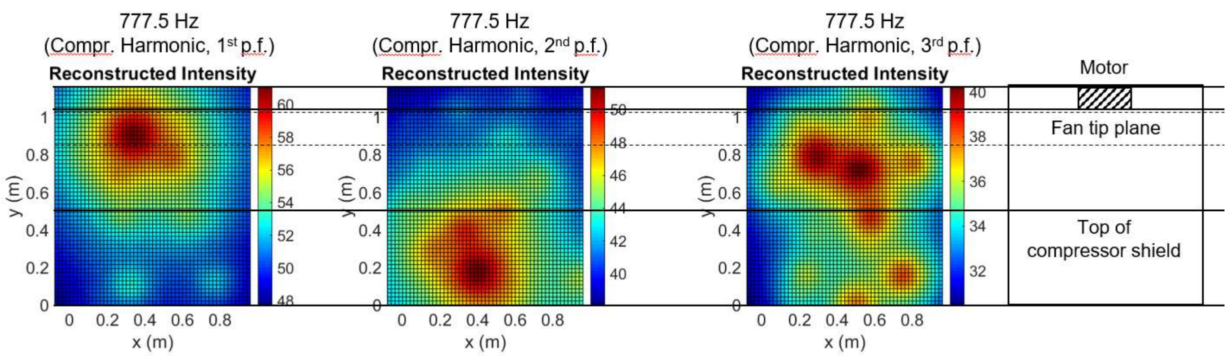

Figure 9: Fan and compressor running: reconstructed sound field of the 1st, 2nd, and 3rd partial field at a compressor harmonic (777.5 Hz).

Shown in Fig. 10 are the first three partial fields of the reconstructed sound field of an unidentified source (800 Hz) when only the fan is running. The bulk of the sound radiation in this case appears to be radiating from the region near the top of the unit.

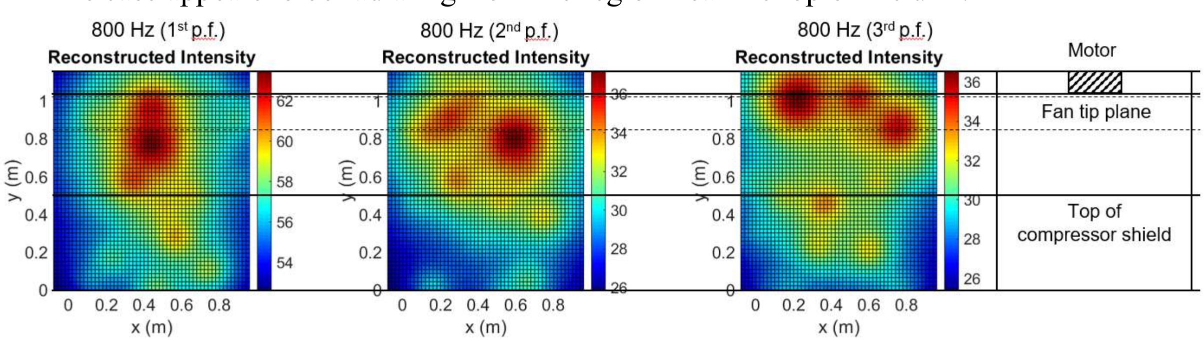

Figure 10: Only fan running: reconstructed sound field of the 1st, 2nd, and 3rd partial field of an identified source (800 Hz).

Intensity probe measurements were taken to compare with the predicted sound field reconstructions while only the fan was running and while both the fan and compressor were running. Intensity probe measurements were taken at 81 locations in a 9 x 9 measurement grid 10 cm away from the unit. Each measurement was 10 cm apart in a square array. For comparison, the total sound field was reconstructed at those same 81 locations. In both the intensity measurements and the reconstruction results, the intensity was interpolated between the 81 locations. The intensity is also integrated around 3 data points above and below 45 Hz and 545 Hz. Since the frequency resolution is 2.5 Hz, the results below represent an intensity integration from 39-51 Hz and from 539-551 Hz, respectively.

For the case when only the fan was running in Fig. 11, the intensity probe measurements and sound field reconstruction were mostly in good agreement at 45 Hz and 545 Hz. At 45 Hz (blade passage frequency), the sound source was localized near the top of the unit, while at 545 Hz (36th harmonic of the motor), the sound source was localized near the bottom of the unit. Since the motor is in fact on the top of the unit, the localized sound source near the bottom is likely due to structure-borne radiated sound.

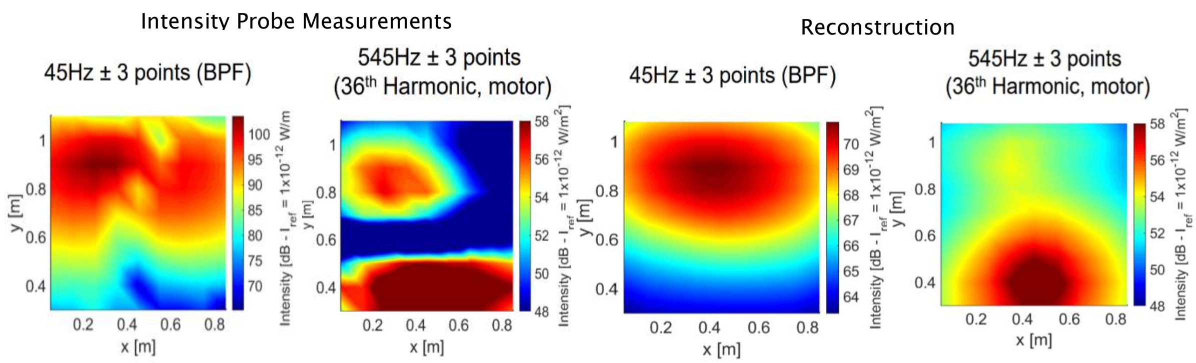

Figure 11: Only fan running: A comparison of the intensity probe measurement results and total sound field reconstructed at 45 Hz and 545 Hz.

In the case when both the fan and compressor were running in Fig. 12, again the intensity probe measurements and sound field reconstruction were mostly in good agreement. In both Figs 11 and 12, it can be seen that the intensity probe measurements are generally higher in level than the reconstructions. This is likely due to the fact that the intensity probe measurements also measure near field effects while the reconstructions do not.

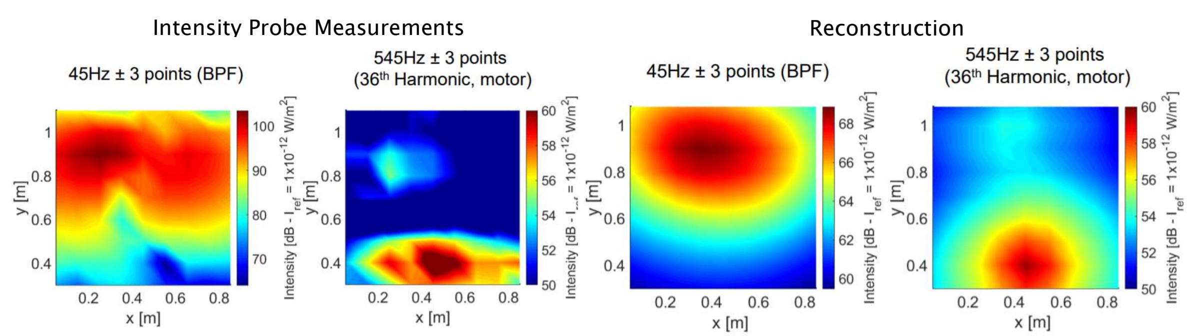

Figure 12: Fan and compressor running: A comparison of the intensity probe measurement results and total sound field reconstructed at 45 Hz and 545 Hz.

4. CONCLUSIONS

In the present work, it has been shown that the combination of the Arbitrary Source Location (ASL) model and the Wideband Acoustical Holography (WBH) procedure can provide useful sound field visualizations. These sound field reconstructions were able to localize and distinguish noise sources at relatively low frequencies, such as the fan, motor, and compressor, in an outdoor HVAC unit. Intensity probe measurements were used to compare to the total sound field reconstructions to verify the results.

5. ACKNOWLEDGEMENTS

This work was made possible by the financial support of Carrier Corporation.

6. REFERENCES

1. J. Hald, Wideband Acoustic Holography, *Proceedings of Inter-Noise14*, Melbourne, Australia, pp. 308-320 (November, 2014).
2. T. Shi, Y. Liu, J. S. Bolton, A Comparison of Two Equivalent Source Methods for Noise Source Visualization*, Proceedings of NoiseCon17*, Grand Rapids, MI, USA, pp.1057-1068, (June 2017).
3. T. Shi, Y. Liu, J. S. Bolton, The Use of Wideband Acoustical Holography for Noise Source Visualization*, Proceedings of NoiseCon16*, Providence, RI, USA, pp.479-490, (June, 2016).
4. Y. Liu and J. S. Bolton, The Use of Non-Collocated Higher Order Sources in the Equivalent Source Method*, Proceedings of Inter-Noise12*, New York, NY, USA, pp.7326-7337, (August, 2012).
5. Y. Liu and J. S. Bolton, Sound Field Reconstruction Using Multipole Equivalent Source Model with Un-Fixed Source Locations, *Journal of the Acoustical Society of America*, 144(5), 2674-2690 (2018).
6. Y. Liu and J. S. Bolton, On the Completeness and the Linear Dependence of the Cartesian Multipole Series in Representing the Solution to the Helmholtz Equation*, Journal of the Acoustical Society of America*, 140(2), EL149-EL153 (2016).
7. M. Lee and J. S. Bolton, Scan-based Near-field Acoustical Holography and Partial Field Decomposition in the Presence of Noise and Source Level Variation*, Journal of the Acoustical Society of America*, Vol. 119, 382-393 (2006).